Engineering Structures 49 (2013) 295–305

Contents lists available at SciVerse ScienceDirect

Engineering Structures

journal homepage: www.elsevier.com/locate/engstruct

Rehabilitation of defected RC stepped beams using CFRP ☆

Hamdy Mohy El-Din Afefy [a,*], Mohamed Hussein Mahmoud [b], Tarek Mohamed Fawzy [b]

[a] Structural Engineering Dept., Faculty of Engineering, Tanta University, Tanta, Egypt
[b] Faculty of Engineering, Tanta University, Tanta, Egypt

ARTICLE INFO

Article history:
Received 26 August 2012
Revised 2 November 2012
Accepted 12 November 2012
Available online 25 December 2012

Keywords:
Beam
Carbon fiber reinforced polymer (CFRP)
Ductility
Experimental study
Rehabilitation
Restoration
Stepped beam
Stiffness
Strengthening

ABSTRACT

Stepped beam is an example of non-prismatic beams that provides stress concentration at the stepped joint and requires an adequate detailing for such joint in order to avoid premature failure. Although, fiber reinforced polymer (FRP) materials are widely used for the strengthening and retrofitting of concrete structures and bridges, the choice of effective FRP-strengthening configuration for special RC members such as stepped beams is still a challenging issue. This paper presents both experimental and analytical investigations undertaken to evaluate the ability of externally bonded (EB) CFRP strips and sheets to restore the ultimate capacity of defectively detailed stepped beams. Five beams were reinforced with insufficient bond length flexural reinforcement and were designed to be failed by de-bonding. Two additional beams were adequately reinforced with two different correct details and served as control specimens. Before testing, four defected beams were strengthened using hybrid system of both EB-CFRP strips and sheets with different configurations. The strengthening strategy of these beams was based on analyzing their stepped joints using strut-and-tie model with all possible arrangements of tension and compression members and then applying the strengthening strips and sheets parallel to the obtained tension ties. Test results showed that, in contrary to the observed behavior of the correctly detailed beams, the un-strengthened defected beam exhibited premature splitting failure due to slippage of the main reinforcement and, its load carrying capacity was decreased by about 77% compared with that of the correctly detailed beam. However, strengthening the defected beams with EB-CFRP had not only restored the defected beams flexural capacity but also, prevented the early steel reinforcement de-bonding and consequently enhanced the flexural performance of the strengthened beams. Finally the most efficient EB-CFRP strengthening configuration is proposed.

© 2012 Elsevier Ltd. All rights reserved.

1. Introduction

Stepped beam is an example of non-prismatic beams that can be used to support a split-level floor. This application is commonly used in theaters and in private housing for aesthetic reasons. The stepped beam provides additional need for reinforcement detailing to fulfill the stress concentration at the stepped joint.

The well-known advantages of fiber-reinforced polymer (FRP) composites over other strengthening materials make them a good choice for civil engineering applications. These materials can be designed and used in the form of laminates, rods, dry fibers (sheets) adhesively bonded to the concrete, wet lay-up sheets mounted on the surface, or near surface mounted bars or laminate strips in the concrete cover [1].

Over years, a large numbers of studies on the behavior of CFRP-strengthened beams have been conducted to have a better understanding for their behavior under different loading conditions along with to develop the best technique of applying the CFRP fabric sheets and/or strips.

Many drawbacks associated with the application of the CFRPs attributed to the characteristics of currently available commercial CFRP strengthening systems. Although CFRPs have high strength, they are very brittle. When loaded in tension, FRPs exhibit a linear stress–strain behavior up to failure, without exhibiting a yield plateau or any indication of an impending failure. As FRPs behave differently than steel, they consequently suffer from a significant loss in beam ductility, particularity when CFRPs are used for flexural strengthening of RC beams [2–7].

Several studies were conducted in order to identify the methods of preventing premature failure with the aim of improving the load carrying capacity and ductility of RC beams. Researchers studied the use of end anchorage techniques, such as U-straps, L-shape jackets, and steel clamps, for preventing premature failure of RC beams strengthened with FRP sheets [8–10].

☆ The experimental work had been conducted at Tanta University's Concrete and Heavy Structures laboratory.

* Corresponding author. Address: 34 Ahmed Farouk Ali Ezzat, Smouha, Alexandria, Egypt. Mobile: +20 106 177 3174, tel.: +20 3 4298 793.

E-mail addresses: hamdyafefy@hotmail.com (H.M. Afefy), m_hussein_20@yahoo.com (M.H. Mahmoud), telakrat1@yahoo.com (T.M. Fawzy).

0141-0296/$ - see front matter © 2012 Elsevier Ltd. All rights reserved.
http://dx.doi.org/10.1016/j.engstruct.2012.11.013

Aidoo et al. [11] presented an experimental study on the behavior of eight reinforced concrete bridge girders taken from a decommissioned interstate bridge and retrofitted with three different carbon–fiber-reinforced polymer systems subjected to monotonic loading to failure with and without significant fatigue conditioning. Ehsan et al. [12] verified that the attachment of CFRP laminates with edge strip plates had substantially influenced the performance of CFRP-strengthened beams. In addition, the important practical issues that were encountered in strengthening of beams with different type and different thicknesses of fiber reinforced polymer were addressed in [13]. Hence a simple method of applying fiber reinforced polymer for strengthening the beam with different fiber reinforced polymer types with different thicknesses was proposed.

In addition to the practical experience for choosing the strengthening configuration, design guidelines for FRP reinforced concrete structures were stipulated [14]. The application of the strut and tie model in the analysis and design of non-prismatic reinforced concrete beams was also investigated [15,16].

In the current study, four CFRP strengthening configurations covering two models were considered based on the strut-and-tie model for the stepped beam under monotonic incrementally 4-point loading system. The proposed strut-and-tie models were constructed based on the cracking patterns of three un-strengthened stepped beams with defected and corrected reinforcement detailing. The strengthening configurations were applied on base defected stepped beams. The target of the current study was to check the adequacy of the chosen CFRP strengthening configurations to restore the ultimate capacity of the defected stepped beams.

1.1. Strut-and-tie model

Structural members may be divided into regions called B-regions, in which beam theory applies, including linear strain distribution, and other regions called discontinuity regions, or D-regions, adjacent to geometric discontinuities and abrupt changes in cross section as in case of stepped beam, where beam theory does not apply. The strut-and-tie model represents a rational flow of forces from the loads through the D-region to the support points. Frequently, the strut-and-tie model can be determined by testing a similar member or from an elastic stress analysis. As a sign conventions, principal compression stresses act parallel to the dashed lines, which are known as compressive stress trajectories (struts). Principal tensile stresses act parallel to the solid lines, which are called tensile stress trajectories (ties). Fig. 1 shows the components of the strut-and-tie model.

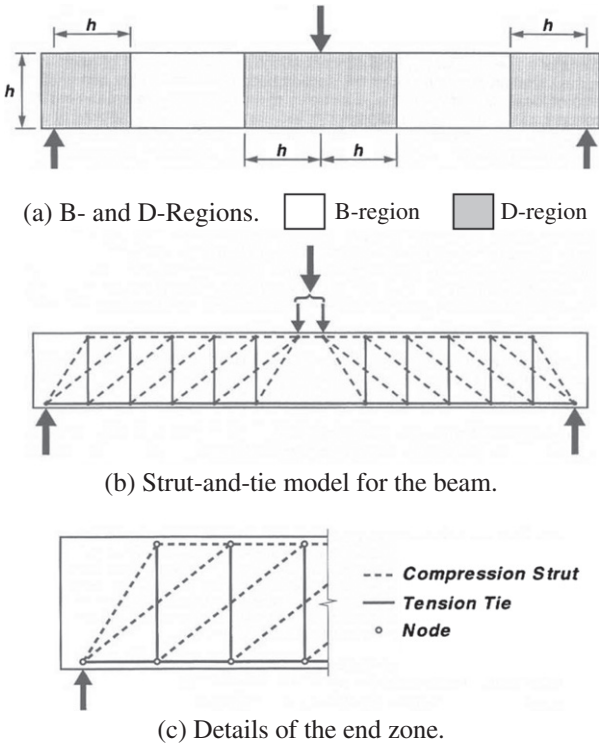


Fig. 1. Components of the strut-and-tie model.

2. Experimental work program

2.1. Test beams

A total of seven beams were fabricated and casted then tested up to failure. The beams were divided into two groups; the first group which contained three beams representing un-strengthened beams, and the second group contained four beams representing the CFRP-strengthened beams. All the beams had the same concrete dimensions where the total length of the beams was 2600 mm while the center to center span was 2400 mm. The beams cross-section was 150 mm width by 300 mm total depth. The main steel reinforcement of the beams was two high tensile steel bars of 12 mm diameter, while the secondary steel was two high tensile steel bars of 10 mm diameter. The stirrups were mild steel bars of 8 mm diameter and spaced every 100 mm in the shear spans and 150 mm in the middle part between the two loading points. The stepped beams were consisted of two portions; upper portion and lower portion.

Fig. 2 shows the concrete dimensions along with the reinforcement detailing for the defected beams. This reinforcement detailing was used for the control beam, B0, of the first group in addition to all beams of the second group. Fig. 3 shows the detailing of the stepped joints for the remaining two beams for the first group, BI, and BII. Additional diagonal stirrups were provided in case of beam BII to carry out the splitting tensile force developed by the resultant of the bar tensile force [17].

In the current study, the test results of the un-strengthened beams were implemented to trace the strut-and-tie model for the stepped beam. The strengthening strategy adopted in the current study was to strengthen the beam in the tie directions using CFRP sheets or strips while the struts were carried out by concrete. Based on the test results of the un-strengthened beams, two strut-and-tie models were presented; Model I and Model II as shown in Fig. 4.

The second group represented the CFRP-strengthened beams. It contained four beams covering the aforementioned two proposed strut-and-tie models as shown in Fig. 4. Beam BS1 represented strengthened configuration complies with Model I while the strengthening configuration used for beams BS2, BS3 and BS4 complies with Model II. A concrete haunch was used in beam BS4 in order to mitigate the stress concentration on the joint, refer to Fig. 3.

2.2. CFRP strengthening schemes

Four beams were strengthened using carbon–fiber-reinforced polymers, CFRP, in accordance with ACI 440.2R-08 recommendations [18]. The strengthening schemes are demonstrated in Fig. 5. Since the adopted strengthened joints are considered as bond-critical application, surface preparation requirements should be based on the intended application of the CFRP system. The concrete surface was prepared with abrasive techniques. The sharp corners were rounded to a minimum of 12 mm radius to prevent stress concentration in the CFRP system.

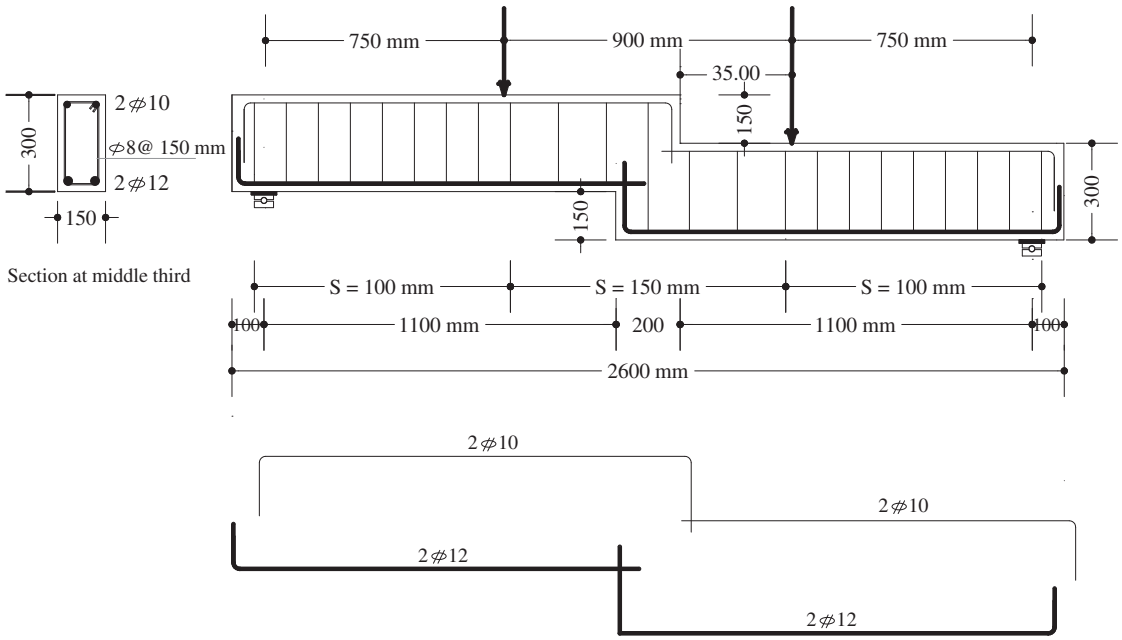


Fig. 2. Concrete dimensions and reinforcement detailing of the control beam (B0) and the base beams of the strengthened beams.

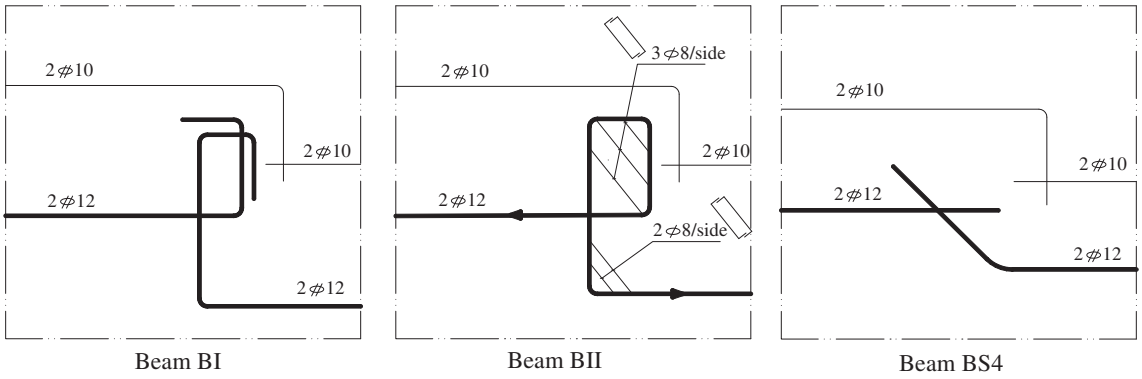


Fig. 3. Reinforcement detailing of stepped part for selected beams.

The common feature of the four strengthened beams was that all beams were strengthened using CFRP strips of dimensions 25 mm width, 1.2 mm thickness and 1200 mm length extended from the tension side of the upper portion to the lower portion and centered at the middle part of the beam. These CFRP strips were mounted at both faces of the beam and were used to compensate the insufficient bond length of the main tension steel of the upper portion.

For beam BS1, two 100 mm width by 0.13 mm thickness orthogonal CFRP sheets were used at the stepped part in order to trace the main ties according to strut-and-tie Model I. Both layers were U-shaped, while the horizontal sheet extended 700 mm along the beam axis and the vertical U-shaped extended 425 mm perpendicular to the beam axis. Finally, two 100 mm width anchorage U-shaped sheets were used at the both ends of the CFRP strips in order to prevent the premature peeling of the strips in addition to the horizontal sheet [19,20]. The vertical sheet had a double duty, in addition to strengthen the beam in the vertical direction, it worked as U-shaped anchorage for the horizontal strips [21]. Strengthening configuration complied with strut-and-tie Model II was used for beams BS2, BS3, and BS4. For beam BS2, one 100 mm width CFRP sheet was used to strengthen the joint in the vertical direction while an inclined 100 mm CFRP sheet at 45° was used to trace the inclined tie as shown in Fig. 5. A horizontal 100 mm U-shaped sheet was used for beam BS3. In addition, the inclined CFRP sheet of beam BS2 was replaced by CFRP strips for beam BS3. The considered configuration of beam BS4 was similar to that of beam BS3 except that a concrete haunch was used in case of beam BS4. In all cases, a 100 mm width U-shaped anchorage sheets were used at both ends of the CFRP strips.

Regarding to the thickness of the epoxy used in the strengthening process, the homogeneously mixed epoxy adhesive was first applied to the concrete substrate with an average thickness of 1 mm by means of a steel trowel and leveled by scraping. The cleaned and completely dried CFRP strip was then coated with the epoxy adhesive in a roof shape by means of a special shaped spatula with an average thickness of 2 mm. A 1.2 mm thickness spacer was used to control the final thickness of the epoxy adhesive.

2.3. Material properties

2.3.1. Concrete

The concrete used was normal strength concrete of 30 MPa target strength, which was the average of three standard cubes of 150 mm

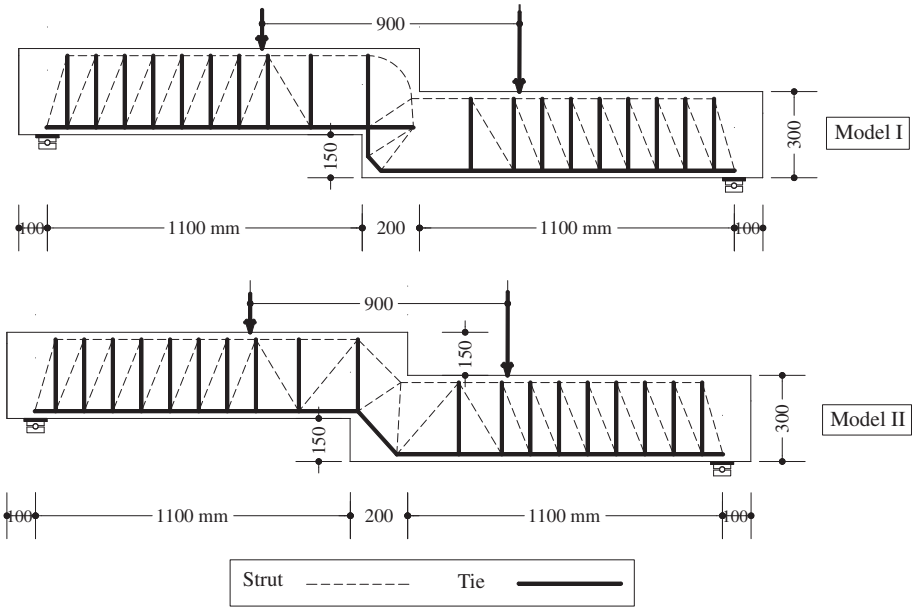


Fig. 4. Adopted strut-and-tie models.

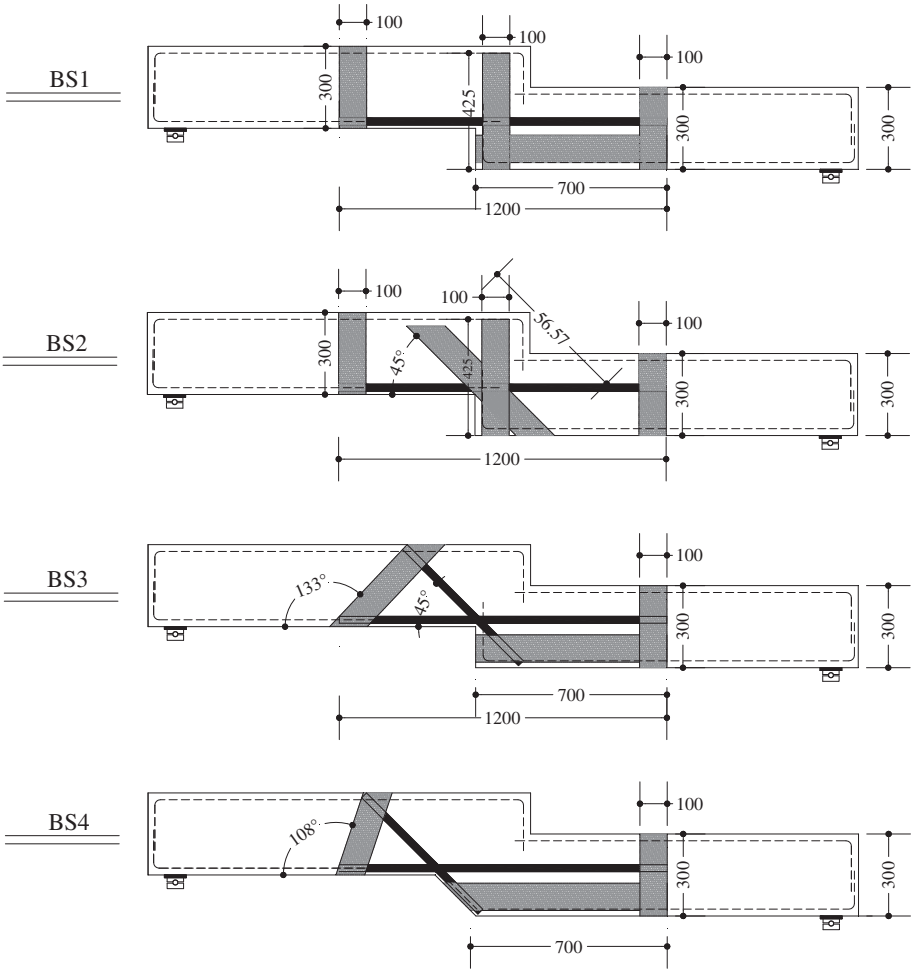


Fig. 5. Strengthening configurations using CFRP sheets and CFRP strips for the strengthened beams.

side. The concrete mix contained crushed pink limestone (type 1) as a coarse aggregate with maximum aggregate size of 10 mm while the sand was supplied from a local pit nearby the site. The volumes of limestone and sand in one cubic meter were 0.8 and 0.4, respectively. The cement used was normal Portland cement (Type I) with 350 kg/m^3 cement content and the water–cement ratio was kept

Table 1
Mechanical properties of CFRP material.

Criteria	CFRP strips	CFRP sheets	Epoxy (for strips)	Epoxy (for sheets)
Tensile strength (MPa)	2800	3500	30	30
Modulus of elasticity (GPa)	165	230	12.80	21.40
Failure strain (%)	1.70	1.50	1.0	4.80
Thickness (mm)	1.2	0.13	–	–

as 0.4. At the time of testing, the actual concrete strength for each beam was obtained as the average of three standard cubes that were tested at the same time of testing the beam.

2.3.2. Reinforcing steel

The longitudinal steel bars were high tensile steel of 400 MPa as the yield strength, while the maximum tensile strength was 600 MPa. The transverse steel was mild steel of 240 MPa yield strength and 350 MPa maximum tensile strength. The modulus of elasticity for both types of reinforcements was 200 GPa.

2.3.3. CFRP sheets, strips and epoxy adhesive

Table 1 shows the mechanical properties for both CFRP strips and fabric sheets along with the epoxy resins as provided by the manufacturer.

2.4. Test setup, test procedure and instrumentation

One bay of three-dimensional steel frame as presented in Fig. 6 was equipped then used to carry out the testing. A 100 mm LVDT was used in order to measure the vertical deflection at mid-span point of the beam. While, 10 mm strain gauges were used to measure the developed strains in reinforcement at the tension sides for upper and lower portions of the beam and the tensile strains in the CFRP sheets and strips as well. In addition, a 50 mm gauge length Pi-gauge was used to measure the deformation at the concrete compression side for the lower portion. Hence, the concrete compressive strain can be obtained. The beam was loaded at two points at both portions of the beam through a loading steel beam. Therefore, in several steps the beam was loaded up to failure. The load on the beam was measured by a load cell of 600 kN capacity. A laser level was used to ensure the coincidence of the axes of the beam, load cell and the loading beam before testing.

After each loading step, the vertical mid-span deflection, the Pi-gauge readings, the strains in main steel for upper and lower portions of the beam in addition to the developed tensile strain in the CFRP sheets and strips were recorded. The loading rate for all beams ranged from 0.1 to 0.2 kN/s. An automatic data logger unit (TDS-102) had been used in order to record and store data during the test for load cell, steel strain gauges, CFRP strain gauges, Pi-gauges, and LVDT.

3. Results and discussion

Table 2 summarizes the recorded failure characteristics after complete collapse of all beams. In the following clauses, the criteria most related to the failure modes for un-strengthened beams and the CFRP-strengthened beams are discussed in detail. The considered criteria includes the mode of failure, load–deflection relationship, cracking load, ultimate capacity, toughness and initial stiffness, concrete compressive strain, ultimate developed strains in the main reinforcing bars at both portions of the beam, and ultimate developed tensile strains in the CFRP strips.

3.1. Mode of failure

The failure mode of beam B0 was noticed to be sudden splitting failure at the end of the main tension reinforcement for the upper portion. The concrete section sustained loading till it reached its tensile capacity, then the tension force was delivered to the tension steel. Due to the insufficient bond length of the main tension steel, it pulled out the concrete leading to tearing off the beam into two parts. The failure of beam BI was flexural failure where cracks began to appear at the tension side of the kink of the stepped joint at a vertical load of about 24.9 kN. Increasing the applied load further led to growing the propagation of the inclined cracks at the stepped joint till the occurring of the complete collapse of the

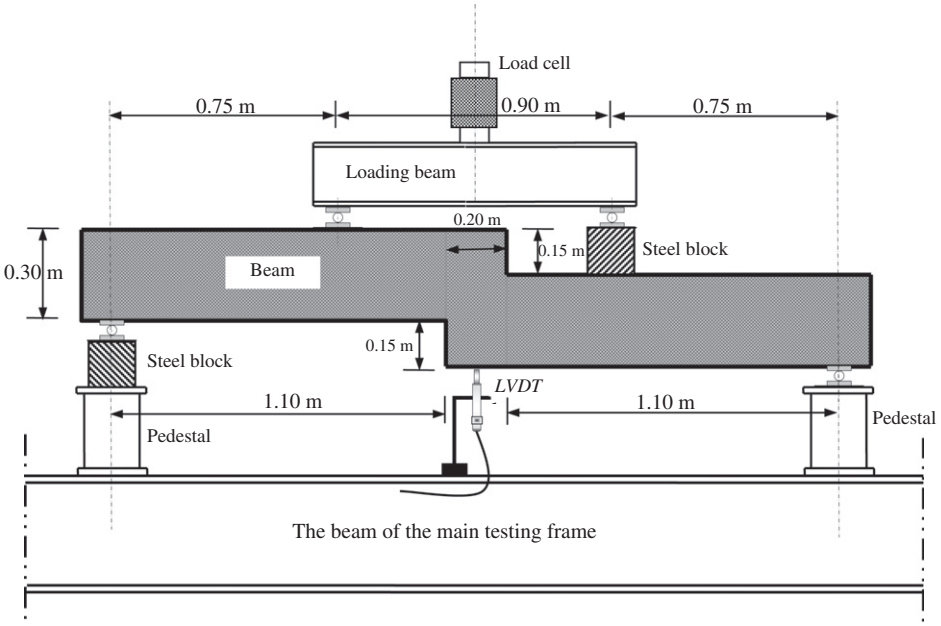


Fig. 6. Test setup.

Table 2
Experimental results and failure characteristics of all beams after complete collapse.

Group No.	Beam	Cube strength (MPa)	Failure load (kN)	[a]Rate of increases in failure loads compared to B0	Toughness (kN mm)	Maximum deflection (mm)	Maximum tensile strain at the lower portion, micro-strain	Maximum tensile strain at the upper portion, micro-strain	Maximum tensile strain at the hl CFRP strip at mid-point, micro-strain	Mode of failure
1	B0	29.5	12.23	–	90	10.7	90	−812	–	Bar slippage
	BI	31.7	50.03	3.09	867	24.4	1852	1453	–	Flexural failure
	BII	31.5	54.28	3.44	915	26.5	1401	1233	–	Flexural failure
2	BS1	30.3	41.66	2.41	521	15.6	898	612	2952	Rupture of the vertical CFRP sheet followed by de-bonding of the horizontal CFRP strip leading to rupture of the end anchorage sheets
	BS2	30.5	62.03	4.07	726	15.7	1366	1168	4383	Rupture of both inclined and vertical CFRP sheets followed by de-bonding of the horizontal CFRP strip leading to rupture of the end anchorage sheets
	BS3	31.9	57.94	3.74	610	14.7	1187	1086	3176	De-bonding of the horizontal CFRP strip followed by de-bonding of the inclined strip leading to rupture of the end anchorage sheets
	BS4	32.2	88.80	6.26	1140	19.0	2384	1904	4207	De-bonding of the horizontal CFRP strip followed by de-bonding of the inclined strip leading to rupture of the end anchorage sheets

[a] Rate of increase in the failure load $= \frac{P_{u(B_1)} - P_{u(B_0)}}{P_{u(B_0)}}$, $P_{u(B_0)}$ refers to the failure load of beam B0, $P_{u(B_1)}$ refers to the failure load of beams BI, BII, BS1, BS2, BS3, and BS4, respectively.

beam in flexural mode of failure. Using of diagonal stirrups inside the stepped joint of beam BII hindered the appearance of the cracks where it began to appear at a vertical load of about 31.5 kN. The beam BII showed similar behavior as that of beam BI till failure except that the propagation of cracks was less than that of beam BI.

Cracks began to appear at the stepped joint of beam BS1 at a vertical load of about 34 kN followed by initiation of the CFRP vertical sheet rupture. Increasing load further led to de-bonding of the horizontal CFRP strip till the rupture of end anchorage occurred. As for beam BS2, cracks began to appear on the concrete surface at a vertical load of about 43 kN then diagonal cracks appeared at the stepped joint at a vertical load of about 49 kN followed by rupture of the diagonal CFRP sheet followed by rupture of the vertical CFRP sheet. Increasing load led to de-bonding of the horizontal CFRP strip followed by rupture of the CFRP anchorage U-shaped. The failure of beam BS3 was characterized by the de-bonding of both inclined and horizontal CFRP strips. Increasing vertical load further led to rupture of the CFRP anchorage sheets. The failure of beam BS4 was triggered by the de-bonding of the inclined CFRP strip followed by rupture of the horizontal CFRP sheet. At the failure state, both horizontal and inclined CFRP strips were de-bonded.

The failure modes of the CFRP-strengthened beams showed that it is better to use either CFRP sheet or CFRP strip diagonally at the joint which complies with the strut-and-tie Model II. Strengthening configuration adopted for beam BS2 showed the best results which mean that the used CFRP sheets and strips traced the developed ties on the joint adequately. The strengthening configurations for both beams BS3 and BS4 were the same except that the beams BS4 had a haunch. This haunch changed the failure characteristics significantly. It delayed the appearance of cracks, changed the sequence of failure for the CFRP laminates, and increased the ultimate capacity. The beam BS3 showed similar failure mechanism as that of beam BS4 except that the corresponding vertical load was smaller than that of beam BS4, Fig. 7 shows the failure patterns for both un-strengthened and CFRP-strengthened beams.

3.2. Load–deflection response

Fig. 8 shows the relationship between the total vertical load and the corresponding mid-span deflection for all beams. The un-strengthened beams, B0, BI and BII showed the same behavior till the failure of defected beam, B0. The appearance of the first crack for beam B0 was associated with the de-bonding of the main tensile steel of the upper portion leading to increased deflection with slightly decreased loading. Both beams BI and BII showed almost the same load–deflection behavior till the appearance of the first crack for beam BI at a vertical load of about 24.9 kN. Subsequently, the behavior began to differ where beam BII exhibited lower deflection compared to that of beam BI at the same loading level.

For the CFRP-strengthened beams, it can be seen that all strengthened beams showed lower corresponding deflection at the same vertical load compared to that of un-strengthened beams. In addition, the response of the CFRP-strengthened beams showed significant variation for the whole post-cracking behavior. The highest deflection was noticed for beam BS1 while the lowest deflection was observed for beam BS4 at the same loading level.

The load–deflection response was noticed to be linear till the appearance of the first crack for un-strengthened beams. While, the vertical loads corresponding to the visible cracks for the CFRP-strengthened specimens were located on the nonlinear portion of the load–deflection relationship. This can be attributed to the initiated cracks beneath the CFRP layers.

3.3. Ultimate capacity, initial stiffness, ductility and cracking load

Table 2 shows the ultimate sustained load at failure for all beams. It can be seen that using insufficient bond length for the main tension steel as for beam B0 could drop the ultimate capacity by about 75.5% compared to the ultimate capacity of beam BI. In addition, using of properly designed inclined stirrups in accordance with the ECP 203-2007 [17] at the joint of the stepped beam BII

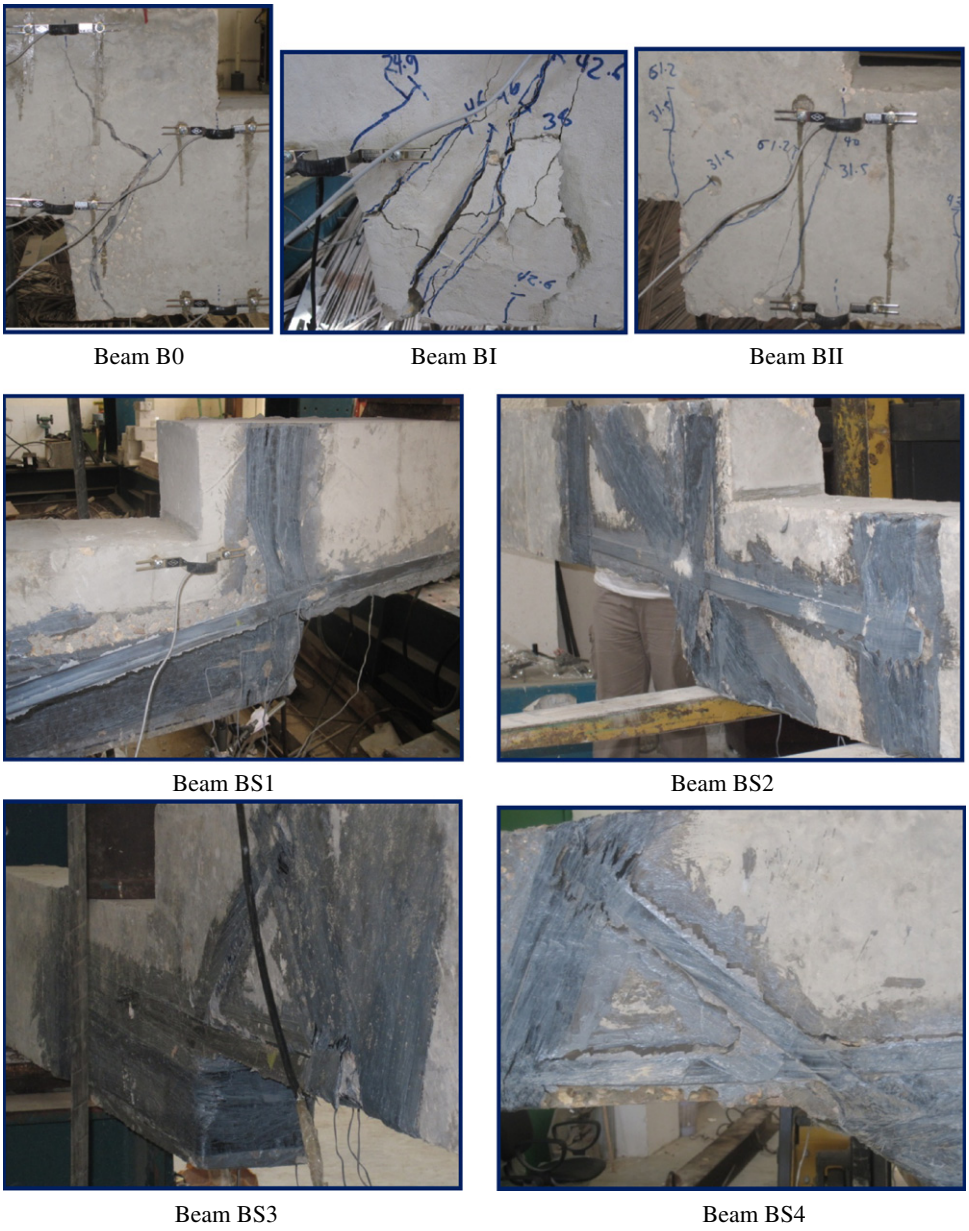


Fig. 7. Failure modes of all beams.

could enhance the ultimate capacity by about 8.5%, compared to that of beam BI.

In order to verify the efficiency of the CFRP strengthening configuration, the ultimate capacities of the four CFRP-strengthened beams were compared to that of beam BII. The comparison showed that the CFRP strengthening configuration of beam BS1 did not restore the full ultimate capacity of the properly detailed beam when using CFRP system on a defected beam detailed as beam B0. The ultimate capacity of beam BS1 was lower than that of beam BII by about 14.2%. On the other hand the ultimate capacities of beams BS2, BS3 and BS4 showed higher capacities by about 14.2%, 6.7% and 63.5%, respectively, compared to that of beam BII. In sum, The CFRP strengthening configuration can either restore the ultimate capacity of defected stepped beam or not, according the efficiency of the adopted strengthening configuration.

Based on the strut-and-tie model, the ultimate capacity of the defected beam could be exceedingly restored by about 15%. In addition, the proposed model, Model II, showed its superiority over Model I, where the higher ultimate capacity was provided by beam BS2. This can be attributed to the efficiency of the inclined CFRP sheet in restraining the inclined cracks better than the orthogonal sheets.

It is worth mentioning that the higher capacity of beam BS4 was not owing to the strengthening configuration only but also to the adopted haunch at the joint, because the strengthening configuration for both beams BS3 and BS4 was that same. But, the difference in the ultimate capacities was significant.

Another comparison criterion for all beams is the initial stiffness. The initial stiffness is the slope of the first part of the load–deflection curve. Fig. 9 shows comparisons among all beams based on normalize initial stiffness. It can be seen that the un-strengthened beams have approximately the same value. On the other hand, all strengthened beams showed higher values compared to that of beam BII. In addition the variations of the initial stiffness for all CFRP-strengthened beams were noticeable. Numerical results for the initial stiffness could be easily obtained from the load–deflection relationships for all beams.

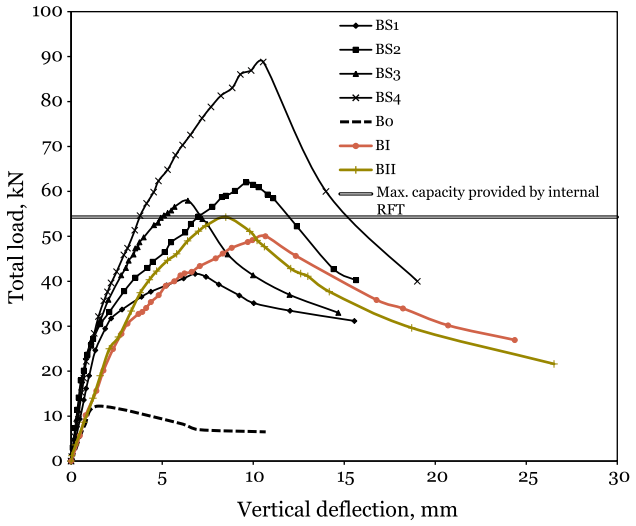


Fig. 8. Vertical load versus mid-span deflection for all beams.

Ductility may be broadly defined as the ability of a structure to undergo inelastic deformations beyond the initial yield deformation with no decrease in the load resistance. Toughness of the system can be defined as the maximum energy that can be sustained by the system up to failure. It can be used as an indicator for the ductility where higher toughness means higher dissipation of energy, until the failure occurred leading to higher ductility. The toughness can be defined as the area under the load–deflection curve. Fig. 9 shows comparison among all beams from the normalize toughness viewpoint. Inspite that the normalization was carried out based on the toughness of beam BII, beam BI showed slight decrease in toughness compared to that of beam BII. It can be concluded that all CFRP-strengthened beams exhibited lower toughness except beam B4 that showed higher toughness compared to that of beam BII. The higher toughness of beam BS4 could be attributed to not only the CFRP strengthening configuration but also to the effect of using concrete haunch.

Another way for ductility comparison is the loading plateau beyond the cracking load till the complete failure since the concrete dimensions, reinforcement detailing and the loading system were the same. Increasing this plateau means higher ductility and vice versa. The measured cracking loads for the CFRP-strengthened beams were noticed to be higher than that of the un-strengthening beams. These cracking loads were about 34 kN, 43 kN, 42 kN, and 56 kN, for beams BS1, BS2, BS3 and BS4, respectively. This can be attributed to the arresting effect of the CFRP configuration.

Fig. 10 shows comparisons among the percentage of cracking load to the ultimate load for all beams. The higher value means lower ductility. Eliminate the value of beam B0 from Fig. 9 and compare their results with the results of Fig. 10 yields the same trend. The highest value in Fig. 10 was for beam BS1 this means that it had the lowest ductility. This result could be obtained from Fig. 9 where the lowest ductility was for beam BS1.

Inspite that beam BI showed lower toughness than that of beam BII as shown in Fig. 9, it showed higher ductility according to Fig. 10. This can be attributed to the properly detailed stepped joint which hindered the appearance of cracking for beam BII. However, the same trend was noticed for beam BS4. It can be concluded that both schemes can be used as a ductility indicator based on the accuracy of the measured load–deflection responses and the cracking load values.

3.4. Concrete compressive strain at the lower portion

Fig. 11 shows the relationship between the concrete compressive strain at the lower portion of the stepped beams and the ultimate load for all test beams except the defected beam B0. It can be seen that all sharp sloped stepped beams exhibited compressive strain at the lower level of loading. Increasing vertical load led to switching the compressive strain gradually to tensile strain. Increase the load further yielded increased tensile strain up to failure. The un-strengthened beams, BI and BII, along with the CFRP-strengthened beams, BS1, BS2, and BS3, showed the same trend of strain distribution. On the other hand, haunched stepped beam, beam BS4, showed monotonic strain up to failure. The strain was compressive strain from the beginning of loading up to failure. This phenomenon can be explained with the aid of the developed internal forces as shown in Fig. 12. For the sharp stepped beam, the compression resultant of the main steel tension force is inclined by 45° with the horizontal reaching the compressed upper face of the lower portion. The high compression force has developed perpendicular splitting tensile force of about one quarter of such force [17]. Increasing the vertical load resulted in increasing such splitting force leading to switching the compression strain to tensile strain. This observation was clear at the failure pattern of beams BI and BII as given in Fig. 7 where the inclined cracks approached the upper fiber of the compressed zone. On the other hand, the resultant of the internal tensile forces for the haunched stepped beam

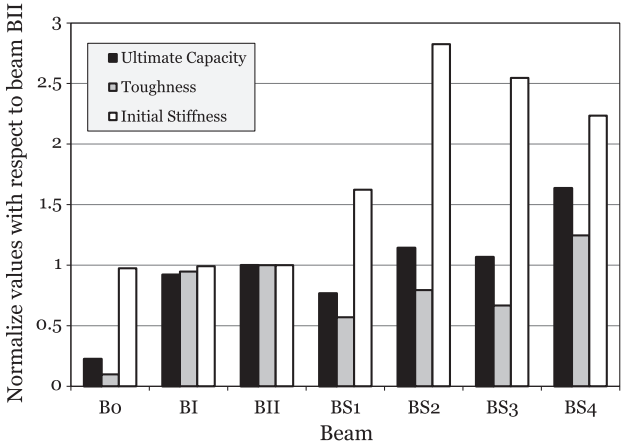


Fig. 9. Comparison among normalizes ultimate capacity, toughness and initial stiffness for all beams.

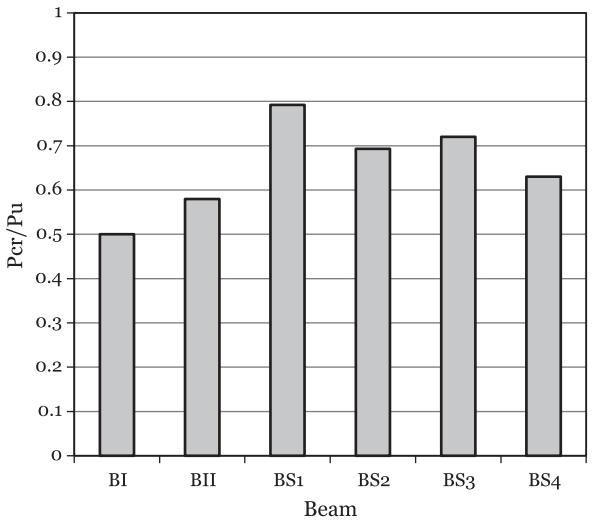


Fig. 10. Percentage of cracking load to the ultimate load for all beams.

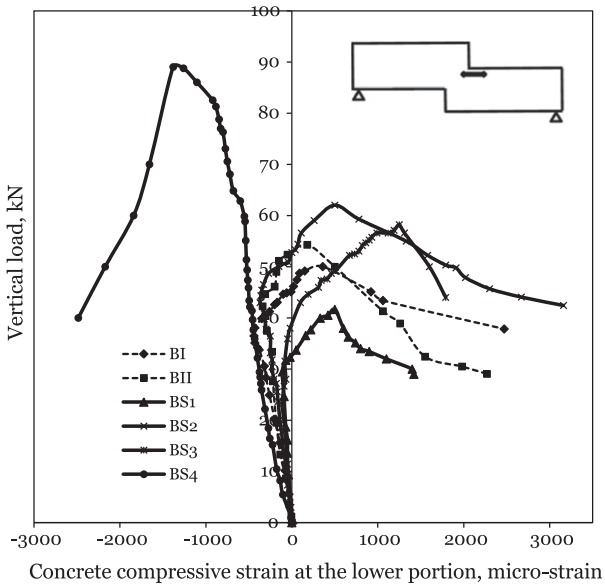


Fig. 11. Vertical load versus concrete compressive strain at the lower portion for all beams.

is directed to the upper kink of the stepped joint which kept the upper portion of the beam under compression strain.

3.5. Ultimate tensile strains

Table 2 shows the recorded maximum developed tensile strains in both tension steel and the CFRP strips at mid-span of the beams. As for the main tension steel, the common feature was that none of the un-strengthened beams had yielded. In addition, the developed strains in the tension steel for the lower portion were higher than that at the upper portion for the relevant beam. For the defected beam, the main steel of the upper portion had developed a compression strain due to the sudden slippage of the steel bars as a result of insufficient bond length. The CFRP-strengthened beams showed the same behavior of the un-strengthened beams except that the main tension steel of the lower portion of beam BS4 yielded at failure while the main steel of the upper portion approached the yield point at failure.

For the CFRP-strengthened beams, the tensile strains were measured at the mid-point of the horizontal strip for all strengthened beams as reported in Table 2. It can be noted that the measured strains were ranged from 17% to 26% of the failure strain of the CFRP strips. However, the CFRP strips may be stressed beyond that level at different locations away from the measured point. As for the CFRP sheets, it was noticed that for all strengthened beams the CFRP sheets reached the rupture strain on either the strengthening sheet or the anchorage sheet where the CFRP sheets failed due to rupture. However, the developed tensile strains at failure on the CFRP sheets had not been measured.

3.6. Adequacy of the CFRP strengthening configurations

In this part, the adequacy of the strengthening configurations is checked based on the criteria of how they helped to restore the yielding capacity of the internal steel that has insufficient bond length. Based on the measured strain in the horizontal CFRP strip that compensated the insufficient bond length of the internal steel, the recorded ultimate capacity at failure and the actual concrete strength for the beams at the testing day as reported in Table 2, a contribution factor for the internal steel, k, was assumed and evaluated. The factor k represents a contribution factor which is a fraction of the yielding force of the internal steel. Hence, this factor can be used as an indicator of the efficiency of the strengthening configuration where higher value shows that the adopted CFRP strengthening configuration can help to restore the yielding capacity of the internal steel and vice versa.

The main concept was based on the state of equilibrium between the internal moment capacity for the concrete cross-section and the external moment capacity of the entire beam. Here in below, a detailed description for the calculation of the factor k is presented for beam BS1at the critical section of the upper portion.

Based on the equilibrium of the internal forces as shown in Fig. 13 of the equivalent stress block [22]

Total compression force = Total tension force

$$C = T_f + T_s \tag{1}$$

where C is the total compression force carried by concrete, T_f is the tension force carried by the CFRP strip, and T_s is the tension force carried by the internal steel

$$C = 0.8 \times 0.85 f_c' \times \beta_1 c \times b \tag{2}$$

$$C = 0.68 \times 30.3 \times 0.84c \times 150 = 2596.1c$$

$$T_f = E_f \times \varepsilon_f \times A_f \tag{3}$$

where E_f is the modulus of elasticity of the CFRP strip as given in Table 1, ε_f is the measured strain at failure in the CFRP strip, and A_f is the cross-sectional area of the CFRP strip.

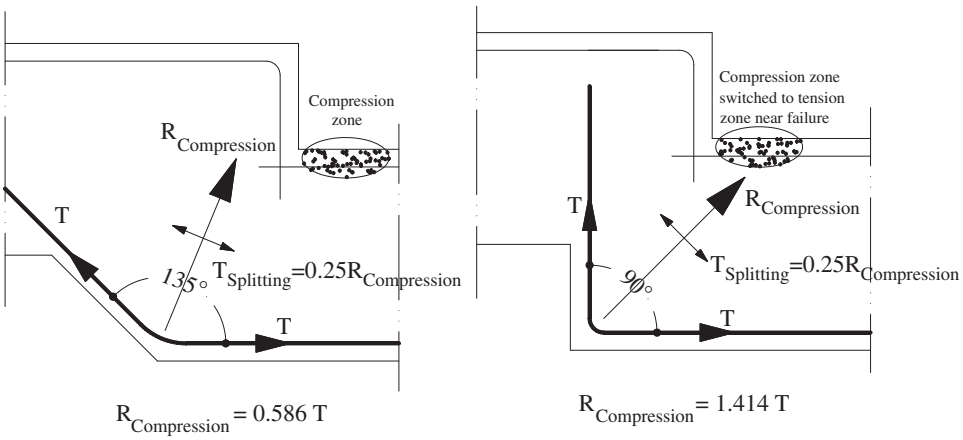


Fig. 12. Force resultant at the stepped joint for the sharp and haunched type [17].

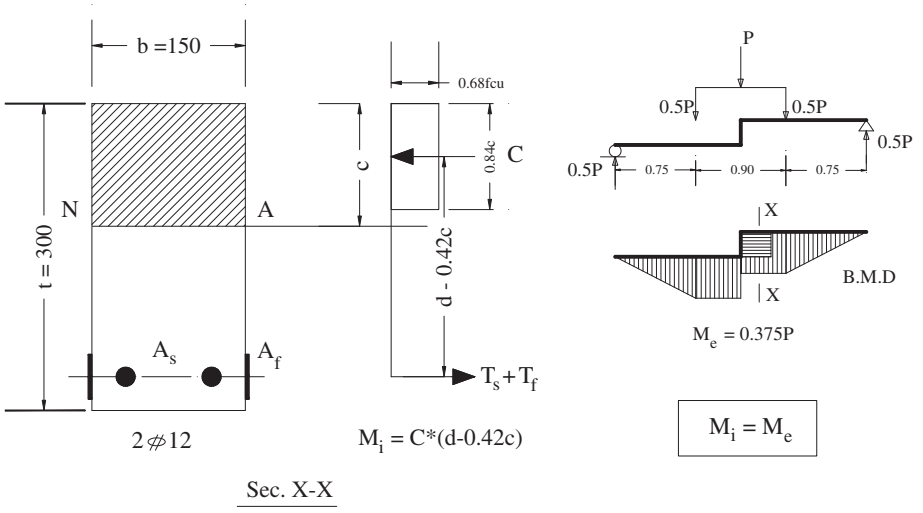


Fig. 13. Internal and external forces at the critical section of the upper portion [22].

Table 3
Contribution percentage of inadequate steel reinforcement due to external CFRP strengthening.

Beam	Contribution factor, k	Actual stress based on measured strain (MPa)	Actual contribution = actual stressed divided by yield stress	Analytical/ Actual contribution
BS1	0.34	122.4	0.306	1.11
BS2	0.53	233.6	0.584	0.91
BS3	0.59	213.6	0.534	1.10
BS4	1	380.8	0.952	1.05

$$T_f = 165,000 \times (2952/10^6) \times 1.2 \times 25 \times 2 = 29224.8\ \text{N}$$

$$T_s = k \times f_y \times A_s \tag{4}$$

where f_y is the yield stress of the steel reinforcement, A_s is the cross-section area of the steel reinforcement and k is a contribution factor of the internal steel.

$$T_s = k \times 400 \times 2 \times 113 = 90,400k$$

Substituting the values of Eqs. (2)–(4) in Eq. (1) leads to

$$c = 11.26 + 34.82k \tag{5}$$

$$M_e = 0.375 \times P_u = 0.375 \times 41.66 \times 10^6 = 15,622,500\ \text{N mm}$$

where M_e is the external bending moment and since $M_e = M_i$ then

$$M_e = C \times \left(d - \frac{\beta_1 c}{2}\right) \tag{6}$$

Substituting the values of M_e and C in Eq. (6) and solving the second order equation on c yields $c = 23.12$. Then, substituting that value of c in Eq. (5) yields $k = 0.34$. This means the CFRP strengthening configuration for beam BS1 can help internal inadequately bonded steel to sustain 34% of its yield strength.

Using the same procedure, the contribution factors of the internal steel for beams BS2, BS3, and BS4 are 0.53, 0.59 and 1, respectively. The actual stress in the internal reinforcement can be calculated exactly based on the recorded strain in the internal steel. Hence, the ratio of the theoretical contribution to the actual contribution is reported in Table 3. It can be seen that the theoretical contribution factors are matching the actual contributions within a variations no more than 10%.

4. Conclusions

Based on the studied CFRP strengthening configurations of the defected stepped beam, loading scheme, and according to the used concrete dimensions and reinforcement detailing, the following conclusions maybe drawn:

1. The defects in reinforcement detailing of the stepped beam can cause premature failure with a significant drop in the ultimate capacity up to 77% as the case of beam B0 when compared with beam BII.
2. Based on the proposed strut-and-tie model, the adopted CFRP strengthening system can restore the ultimate capacity of defected beam and outperform the behavior of such beam than the properly detailed stepped beam by about 15%.
3. It is not guaranteed that the CFRP strengthening technique always increases the ultimate capacity of defected beam. The affirmative effect always happens if only the proper configuration is chosen based on rigorous analysis.
4. Using haunch is preferable than sharp changing of the concrete section from the viewpoint of all failure characteristics.
5. The sectional analysis showed good agreement with the experimental results regarding to the restoration of the yielding capacity of defected internal reinforcement of the stepped beams.
6. The performance of beam BS2 is just as promising, if not more so, in the fact that the proposed strengthening configuration that based on the second strut-and-tie model (Model II), was able to increase its load-carrying capacity to 62.03 kN, approximately five times higher than that of the control beam B0.

References

[1] Etman EE. Strengthening of T-section RC beams in shear using CFRP. In: Proceedings of concrete solutions, 14th international conference on concrete repair, Dresden, Germany; 26–28 September, 2011. p. 649–60.
[2] Arduini M, Nanni A. Behavior of pre-cracked RC beams strengthened with carbon FRP sheets. J Compos Constr 1997;1(2):63–70.
[3] Bencardino F, Spadea G, Swamy N. Strength and ductility of reinforced concrete beams externally reinforced with carbon fiber fabric. ACI Struct J 2002;99:163–71.
[4] Lee T, Pan A, Ma M. Ductile design of reinforced concrete beams retrofitted with fiber reinforced polymer plates. J Compos Constr 2004;8(6):489–500.
[5] Saadatmanesh H, Ehsani M. RC beams strengthened with GFRP plates. I: experimental study. J Struct Eng 1991;117:3417–33.

[6] Spadea G, Swamy RN, Bencardino F. Strength and ductility of RC beams repaired with bonded CFRP laminates. J Bridge Eng 2001;6:349–55.
[7] Toutanji H, Zhao L, Zhang Y. Flexural behavior of reinforced concrete beams externally strengthened with CFRP sheets bonded with an inorganic matrix. Eng Struct 2006;28:557–66.
[8] Pham H, Al-Mahaidi R. Prediction models for de-bonding failure loads of carbon fiber reinforced polymer retrofitted reinforced concrete beams. J Compos Constr 2006;10:48–59.
[9] Spadea G, Bencardino F, Swamy RN. Structural behavior of composite RC beams with externally bonded CFRP. J Compos Constr 1998:132–7.
[10] Xiong GJ, Jiang X, Liu JW, Chen L. A way for preventing tension delamination of concrete cover in mid-span of FRP strengthened beams. Constr Build Mater 2007;21:402–8.
[11] Aidoo J, Harriess KA, Petrou MF. Full-scale experimental investigation of repair of reinforced concrete interstate bridge using CFRP materials. J Bridge Eng 2006;11:350–8.
[12] Ehsan A, Sobuz HR, Sutan NM. Flexural performance of CFRP strengthened RC beams with different degrees of strengthening schemes. Int J Phys Sci 2012;6:2229–38.
[13] Murali G, Pannirselvam N. Flexural strengthening of reinforced concrete beams using fiber reinforced polymer laminate: a review. ARPN J Eng Appl Sci 2011;6:41–7.
[14] Pilakoutas K, Neocleous K, Guadagnini M, Matthys S. Design guidelines for FRP reinforced concrete structures. ICE Struct Build 2011;164:255–63.
[15] Tan KH. Design of non-prismatic RC beams using strut and tie models. J Adv Concr Technol – Jpn Concr Inst 2004;2:249–56.
[16] Carmo R, Lopes S. Bending moments in D-regions of reinforced concrete beams. ICE Struct Build 2011;164:239–54.
[17] Egyptian code for design and construction of reinforced concrete structures (ECP 203–2007); 2007.
[18] American Concrete Institute (ACI). Guide for the design and construction of externally bonded FRP systems for strengthening concrete structures. ACI 440.2 R-08, Farmington Hills, Mich.; 2008.
[19] Bilal S, Amal Y, Hage A, Harajli MH. Effect of fiber-reinforced polymer confinement on bond strength of reinforcement in beam anchorage specimens. J Compos Constr 2005;9:44–51.
[20] Sarah L, James O, Oguzhan B. Design considerations of carbon fiber anchors. J Compos Constr 2008;12:608–16.
[21] Hussein M. Strengthening of non-prismatic continuous reinforced concrete beams using CFRP. In: 14th International conference on structural faults and repair, Edinburgh, Scotland, UK; 3–5 July, 2012.
[22] American Concrete Institute, ACI. Building code requirements for structural concrete (ACI 318-11) and commentary. Farmington Hills: ACI; 2011.